

---

# Isometric Graph Neural Networks

---

Matthew Walker Bo Yan Yiyou Xiao Yafei Wang Ayan Acharya  
 LinkedIn

## Abstract

Many tasks that rely on representations of nodes in graphs would benefit if those representations were faithful to distances between nodes in the graph. Geometric techniques to extract such representations have poor scaling over large graph size, and recent advances in Graph Neural Network (GNN) algorithms have limited ability to reflect graph distance information beyond the first degree neighborhood. To enable this highly desired capability, we propose a technique to learn **Isometric Graph Neural Networks** (IGNN), which requires changing the input representation space and loss function to enable *any* GNN algorithm to generate representations that reflect distances between nodes. We experiment with the isometric technique on several GNN architectures for modeling multiple prediction tasks on multiple datasets. In addition to an improvement in AUC-ROC as high as 43% in these experiments, we observe a consistent and substantial improvement as high as 400% in Kendall’s Tau (KT), a measure that directly reflects distance information, demonstrating that the learned embeddings do account for graph distances.

## 1. Introduction

Position information plays an important role in many representation learning architectures. In modeling sequence data, such as sentences (Sutskever et al., 2014) and trajectories (Alahi et al., 2016), the position information of each word and stay point is explicitly captured in the model design with recurrent patterns and mechanisms that preserve long-range sequential structure. Such modeling strategies are based upon the intuitive understanding of the temporal translation invariance and relational inductive bias (Battaglia et al., 2018) commonly observed in sequence data. Studies (Yang et al., 2016; Zeng et al., 2014) have also shown that architectures, such as the Convolutional Neural Networks (CNN), specifically designed for 2D data, such as images, are able to outperform sequence models on natural language processing tasks when position features are encoded. Moreover, by modifying the CNN structure to specif-

ically propagate position (spatial) information, performance is significantly improved on particular object detection tasks (e.g., lane detection) that require a better understanding of the spatial relationship of different pixels (Pan et al., 2018).

This importance applies to learning representations in graphs which has gained a lot of traction among researchers and practitioners alike for the abundance and diversity of graph-structured data, such as molecule networks, social networks, and knowledge graphs. These representation learning approaches can be usually classified into three categories – factorization-based approaches (Belkin & Niyogi, 2002; Ahmed et al., 2013; Ou et al., 2016), random walk-based approaches (Grover & Leskovec, 2016; Perozzi et al., 2014), and neighborhood aggregation and convolution-based approaches (Kipf & Welling, 2017; Hamilton et al., 2017a).

Among them, the Graph Neural Networks (GNN) algorithms that perform neighborhood aggregation and convolution have enjoyed a lot of popularity due to their superior performance on node classification, link prediction, and graph generation tasks (Kipf & Welling, 2017; Hamilton et al., 2017b; Liao et al., 2019). The key idea of GNN is to recursively gather information from neighboring nodes (a.k.a. message passing (Gilmer et al., 2017)), in order to capture multi-hop dependencies by means of aggregation functions and non-linear transformations.

Due to the permutation invariance and isomorphism characteristics in graphs, certain aggregation operations, such as summation, are proven, both theoretically (Xu et al., 2019) and practically (Hamilton et al., 2017a;b), to work better than the others. However, such findings do not preclude the possibility of improving the performance further by incorporating the position or relative ordering<sup>1</sup> of nodes in the graph. On the other hand, Xu et al. (2019); You et al. (2019) observe that GNNs are unable to learn distinct representations of the nodes that reside in different parts of the graph but have identical topological neighborhoods. Therefore, we seek to learn embeddings that are representative of relative distances on the graph, that is, are nearly isometric.

Numerous practical applications of graph embedding algorithms would also benefit if the learned embeddings respect

---

<sup>1</sup>We use concepts such as (relative) position, ordering, and distance interchangeably in the paper.

the relative positions of the nodes in the original graph. One obvious example is that when performing nearest neighbor search over embeddings learned by GNNs, we might like the results to be actual neighbors in the graph sense. In an ontology, preserving the partial order of nodes in the embedding space is usually helpful for reasoning in the latent space (McFee & Lanckriet, 2009; Vendrov et al., 2016). Many use cases of graph data, such as predicting career trajectories in a professional social network (Yan et al., 2019), may also require the preservation of the explicit ordering of nodes, e.g., based on timestamps. Moreover, Veličković et al. (2020) show that GNNs can execute many classical graph algorithms, such as breadth-first search, depth-first search, and shortest path algorithms, based on shared subroutines. The relative position of nodes and graph distances are important concepts within those subroutines, thus discovering embedding algorithms that may preserve graph distances can facilitate further research in this area. Inspired by these findings, we investigate the hitherto unexplored connection between relative node positions/graph distances and the expressive power of GNNs.

Though the positions of the nodes can be explicitly captured in Position-aware GNN (P-GNN) models with the assistance of anchor nodes sampled randomly from the graph (You et al., 2019), such an approach requires a lot of preprocessing (e.g., anchor set selection), introduces additional communications between the nodes and the anchor sets, and is not practically feasible for graphs that evolve rather frequently. On the other hand, simple module-like encoding mechanisms of position information work extremely well for sequence data (Vaswani et al., 2017; Xiao et al., 2014) and spatial feature representation learning (Mai et al., 2020). Motivated by these works, we propose to incorporate a hashing mechanism to encode the position information of the nodes in the graph. Such a hashing mechanism is independent of any specific GNN algorithm and hence can enhance *any* GNN architecture. We justify the utility of the hashing module for encoding positions in the graph by providing a theoretical connection between hashing functions and isometric (distance-preserving) embeddings. Since neural networks can implicitly learn spatial positioning in images (Islam et al., 2020) and navigation tasks (Cueva & Wei, 2018; Banino et al., 2018; Gao et al., 2019), we further investigate whether the GNNs are capable of utilizing the position signals if such a preference is encoded explicitly in the learning objective. The introduction of these two extensions – hashed feature augmentation and the inclusion of the position information in the learning objective – begets **Isometric Graph Neural Networks (IGNN)**. Note that P-GNN tries to minimize distortion and break local isomorphism in a probabilistic manner. In contrast, IGNN addresses these issues using a deterministic formulation that can work with any GNN architecture (see Section 4).

To summarize, the main contributions of our work are the following:

- We connect and expand theoretical results on finding isometric embeddings to graph neural network techniques.
- We provide a prescription for learning near-isometric embeddings using any graph neural network algorithm.
- We demonstrate that applying this technique substantially improves performance in metrics sensitive to network distance in a number of datasets and prediction tasks.

## 2. Related Work

Existing research on GNN has primarily focused on the expressiveness and representational power of different embedding methods. Since the underlying mechanism of GNN variants relies on the message passing and aggregation procedures (Gilmer et al., 2017), a large amount of effort has been invested to discover different aggregation functions to achieve state-of-the-art performance on node classification, link prediction, and graph generation tasks. Empirically, permutation invariant aggregation functions (e.g., mean, sum, max-pooling, min-pooling) are ideal choices for GNNs to learn embeddings in general (Hamilton et al., 2017b;a; Kipf & Welling, 2017). Theoretically, Xu et al. (2019) have established the intricate connection between the discriminative power of GNN and the powerful Weisfeiler-Lehman (WL) graph isomorphism test (Weisfeiler & Lehman, 1968) used to distinguish different graph structures while Chen et al. (2019) have shown an explicit connection between the graph isomorphism test and permutation invariant function approximation.

Besides graph structures, the position, the ordering, and the relative graph distance of nodes have also been taken into consideration for designing expressive GNN architectures as such information is critical in distinguishing topologically identical substructures. Graph kernels (Yanardag & Vishwanathan, 2015; Sugiyama & Borgwardt, 2015) have been used to encode position information in graph representation learning. You et al. (2019) proposed the P-GNN model that incorporates additional message communication using anchor nodes. Compared with graph kernel methods, P-GNN models are closely related to and can be viewed as a generalization of existing GNN models. On a related note, Maron et al. (2019) explored and developed GNN models that incorporated standard Multi-Layer Perceptrons (MLPs) of the feature dimension and a matrix multiplication layer and proved that they have higher expressiveness compared with message passing GNNs while maintaining scalability.

While the goal of these prior works is to develop more expressive GNN models using position information, little theoretical understanding of the mechanism in preserving graph distance (relative node positions) using GNN models has been established. Here we aim to provide theoretical

connections among graph distance preservation, hashing functions, and the learning power of GNNs. Besides, the proposed method can be easily integrated with different GNN architectures to suit different needs.

### 3. Preliminaries

Let  $\mathcal{G} = (\mathcal{V}, \mathcal{E})$  be a graph with a set of vertices  $\mathcal{V}$  and a set of edges  $\mathcal{E}$ , such that  $\forall (v_i, v_j) \in \mathcal{E} | v_i, v_j \in \mathcal{V}$ . Let  $N = |\mathcal{V}|$ . When we refer to the graph distance  $d_{\mathcal{G}}(v_i, v_j)$ , we mean the shortest path on graph edges between nodes  $v_i$  and  $v_j$ .

**Graph Neural Networks.** Graph Neural Network algorithms learn embeddings for the nodes in a graph using both graph structure and node specific features  $\mathbf{X} = (\mathbf{x}_{v_i})_{v_i}$ , where  $\mathbf{x}_{v_i} \in \mathcal{X}$  is the node feature vector corresponding to node  $v_i$ . These algorithms learn a function,  $f : \mathcal{V} \times \mathcal{X} \rightarrow \mathcal{Z}$ , allowing nodes in  $\mathcal{V}$  to be mapped to real-valued vectors  $\mathbf{z} \in \mathcal{Z}$ .

GNN algorithms define a neighborhood for each node in the graph and aggregates messages from these neighbors to update the representation of the current node. Formally, these algorithms iteratively update the representation of a node  $v_i$  by performing aggregation and combinations on the neighborhood  $\mathcal{N}(v_i)$  (the definition of which varies among the algorithms) for  $K$  iterations. The aggregation function  $\mathbf{g}_{v_i}^k = \text{AGG}^k(\{\mathbf{z}_{v_j}^{(k-1)} | v_j \in \mathcal{N}(v_i)\})$  performs the aggregation over a set of vectors  $\{\mathbf{z}_{v_i}^{(k-1)}\}$  for each neighbor of node  $v_i$  from iteration  $(k-1) < K$  to obtain the neighborhood representation of node  $v_i$  for iteration  $k \leq K$ . Typical permutation invariant choices for AGG are mean, max-pooling, and sum (Kipf & Welling, 2017; Hamilton et al., 2017a; Xu et al., 2019). The combination function  $\text{COMB}^k(\mathbf{z}_{v_i}^{(k-1)}, \mathbf{g}_{v_i}^k)$  combines the node representation  $\mathbf{z}_{v_i}^{(k-1)}$  for  $v_i$  at iteration  $(k-1)$  with the neighborhood representation  $\mathbf{g}_{v_i}^k$  for  $v_i$  at iteration  $k$ . Typical choices for COMB are concatenation and summation. In general, a GNN can be represented as

$$\mathbf{z}_{v_i}^k = f((\text{COMB}^k \circ \text{AGG}^k)(\mathbf{z}_{v_i}^{(k-1)}, \{\mathbf{z}_{v_j}^{(k-1)} | v_j \in \mathcal{N}(v_i)\})) \quad (1)$$

where function  $f$ , here, is usually a feed forward neural network (such as a single-layer NN or an MLP). The order in which AGG and COMB are applied may be reversed, such as in the case of Graph Convolutional Networks (GCN) (Kipf & Welling, 2017). The output of a GNN is the  $K$ -th representation of each node, that is,  $\mathbf{z}_{v_i} := \mathbf{z}_{v_i}^K, \forall v_i \in \mathcal{V}$ . Therefore, in GNN algorithms, the parameter set is defined by the formulation of the aggregation, combination, and  $f$  functions.

**Representation Spaces.** Since our objective is to learn representations that are reflective of structural similarity, graph distance, and the similarity inferred by the node features, it

is important to outline the differences among various types of spaces we incorporate distance measures from. How they relate, practically, to implementations of GNNs vary, as certain theoretical results apply to different types of spaces.

**Definition 1.** A *metric space*  $(\mathcal{X}, d)$  is a set  $\mathcal{X}$  endowed with a *distance function*  $d : \mathcal{X} \times \mathcal{X} \rightarrow \mathbb{R}$ , sometimes called a *metric*. This distance function satisfies three key properties for any  $x, y, z \in \mathcal{X}$ : positivity ( $d(x, y) \geq 0$ ), symmetry ( $d(x, y) = d(y, x)$ ), and triangle inequality ( $d(x, z) \leq d(x, y) + d(y, z)$ ).

**Definition 2.** A *finite metric space* is a metric space with a finite number of points.

**Definition 3.** A *Euclidean space* is a metric space with  $\mathcal{X} = \mathbb{R}^n, n \in \mathbb{Z}_+$  characterized by a distance function  $d(\mathbf{x}, \mathbf{y}) = (\sum_{i=1}^n (x_i - y_i)^2)^{1/2}, \forall \mathbf{x}, \mathbf{y} \in \mathbb{R}^n$ .

**Definition 4.** An *embedding* is defined as a map  $f : \mathcal{X} \rightarrow \mathcal{X}'$  between two metric spaces  $(\mathcal{X}, d)$  and  $(\mathcal{X}', d')$ .

**Definition 5.** An embedding is *isometric* iff  $\forall x, y \in \mathcal{X}, d(x, y) = d'(f(x), f(y))$ .

Since graphs with weighted edges are not guaranteed to satisfy the triangle inequality, they are generally not isomorphic to finite metric spaces or the Euclidean space.

**Definition 6.** The *distortion* of an embedding is the smallest value  $\alpha \geq 1$  for which there exists an  $r > 0$  such that  $\forall x, y \in \mathcal{X}$ ,

$$r d(x, y) \leq d'(f(x), f(y)) \leq \alpha r d(x, y) \quad (2)$$

**Finding Isometric Embeddings.** The topic of finding isometric and near-isometric embeddings between spaces is a well-studied problem. The study of embeddings of finite metric spaces into Euclidean spaces is of particular interest to the problem of finding representations for nodes in the graph. To that end, Theorem 1 (Bourgain, 1985; Linial et al., 1995) has been studied in relation to graph neural networks (You et al., 2019; Srinivasan & Ribeiro, 2019). Furthermore, the proof of Theorem 1 is algorithmic, guiding how such an embedding might be constructed.

**Theorem 1.** (*Bourgain Theorem*) Every  $n$ -point metric space  $(\mathcal{X}, d)$  can be embedded in an  $\mathcal{O}(\log n)$ -dimensional Euclidean space with  $\mathcal{O}(\log n)$  distortion.

This promising result is extended by Linial et al. (1995) who show that such an embedding produces the least possible distortion. Unfortunately, the algorithm to find such an embedding takes random polynomial time. Moreover, only when the embedding is achieved on an  $\mathcal{O}(n^2)$ -dimensional space one can adopt a deterministic polynomial-time algorithm. Therefore, both of these alternatives are unappealing for learning representations of large graphs. P-GNN (You et al., 2019) takes inspiration from this approach, but as the

distortion is probabilistic, a given choice of anchor nodes provides no guarantee on the level of distortion. Furthermore, an embedding learned on the input feature space has a distance measure with no connection, in general, to the graph distance.

#### 4. Isometric Graph Neural Network

This section presents the mathematical details of the IGNN framework. As explained in the previous section, in general, it is not possible to learn a representation that preserves the exact distance in a graph. Therefore, for any practical application, one must find an embedding that minimizes the distortion. To that end, we first propose a modular extension of the input representation of the graph data using hashed features. In what follows, we concretely argue for the utility, scalability and injectiveness of such modification of the input features. To reduce the distortion further, we propose a modification to the loss function that explicitly penalizes for large deviations in the embedding space from the distance dictated by the graph. Finally, we discuss the complexity of adopting this prescription during model training.

**Input Representation.** Existing GNN algorithms encode the features of an individual node in two different forms – as a set of dataset-dependent attributes or as a one-hot encoded vector that acts as a proxy for the node identity. Such representations can be realized in a Euclidean metric space trivially, though the distance function associated with such metric space, in general, is completely uncorrelated with the distance inferred by the graph. Therefore, learning an embedding from such representation of the features may not preserve the distances in the graph. Given that any linear transformation  $f(\mathbf{x}) = \mathbf{A}^T \mathbf{x}$ , where  $\mathbf{A}$  is an orthogonal matrix, is an isometric embedding, it is extremely easy to find isometric embeddings between Euclidean spaces, but difficult to find an embedding that respects the distances in the original graph.

To that end, we propose to extend the input feature representations of the nodes in the GNNs by concatenating them with a hash vector. The objective of this enhancement is to increase the dimensionality of the input space so that it helps the GNNs break isomorphisms in the graph and learn a representation that is sensitive to the graph distance. In what follows, we first describe the construction of the hash vector and then argue about the injectiveness it introduces that helps us achieve the objectives mentioned above.

**Definition 7.** A hash vector  $(n, m)$  is an  $n$ -dimensional vector, where each dimension is an  $m$ -bit string generated by a hash function and input seed.

In Algorithm 1, we describe how a hash vector can be generated using a hash function that produces  $m$ -bit strings from an input bit string. We show in Theorem 2 that this

algorithm provides protection from collision as good as generating the hash from  $n$  independent seeds.

---

#### Algorithm 1 Constructing a hash vector

---

**Input:** A hash function  $\mathcal{H}_m : \{0, 1\}^* \rightarrow \{0, 1\}^m$ ; an integer  $n$  defining the dimension of the output vector; the input bit string  $b$  which generates the vector.

**Output:** A hash vector  $h \in \{0, 1\}^{m \times n}$

$h \leftarrow ()$

**for**  $i = 0$  **until**  $n$  **do**

$t \leftarrow \mathcal{H}(b \oplus i); h \leftarrow h \oplus t;$

**end for**

---

**Theorem 2.** Given a hash function  $\mathcal{H}_m : \{0, 1\}^* \rightarrow \{0, 1\}^m$  with a collision probability  $p := p(\mathcal{H}(x) = \mathcal{H}(y) | x \neq y)$ , the collision probability between two hash vectors of dimension  $n$ , generated by Algorithm 1, is  $p^n$ .

*Proof:* Consider two hash vectors  $\{h_{i,1}\}$  and  $\{h_{i,2}\}$ ,  $0 \leq i \leq n$ , generated by input bit strings  $b_1 \neq b_2$ . These hash vectors collide if  $h_{i,1} = h_{i,2}, \forall i$ . Given that  $h_i = \mathcal{H}(h_{i-1} \oplus b)$ , the vector components  $h_i$  are randomly distributed in the hash space. Therefore, the probability of collision is independent for each dimension in the hash vector.

Note that adding the hash vector representation introduces a high degree of injectiveness into the input representation. Xu et al. (2019); Maron et al. (2019) discuss at length how introducing some form of injectiveness into GNN algorithms allows one to break the local structural isomorphisms that prevail in the underlying graph. Compared to these existing approaches that either have probabilistic guarantees or no guarantees on injectiveness, augmentation of the hash representation offers a guarantee of injectiveness up to the collision probability of the hash function and hash vector size. This improvement applies both to datasets with node features and those using one-hot encoded vectors, for which it is very easy to generate unique input seeds for each node.

The approach has several additional advantages. Since the hashes have no security constraints, one may use extremely fast collision-resistant hash functions available for a scalable implementation. The process is also deterministic, guaranteeing that the input representation is reproducible across training runs, inference, and other analysis tasks.

**Learning the Embedding.** The Johnson-Lindenstrauss Lemma (Johnson & Lindenstrauss, 1984), is a weaker result than Theorem 1 (Bourgain Theorem). As described by Linial et al. (1995), the proof is prescriptive, but unfortunately, is still a random polynomial time algorithm. An alternative proof is provided by Frankl & Maehara (1988). The proof shows that there is a random subspace of the original space that satisfies the distortion requirement because the length of projections on random subspaces is normally distributed.

**Theorem 3.** (*Johnson-Lindenstrauss Lemma*) Given  $0 < \epsilon < 1$ , any set of  $n$  points in a Euclidean space can be mapped to  $\mathbb{R}^q$  with a distortion  $\alpha \leq (1 + \epsilon)$  in the distances if  $q > 8 \log n / \epsilon^2$ .

Though the algorithm for which the lemma holds does not scale, it strongly suggests that one can find a mapping between two Euclidean spaces with minimal distortion, which is what is relevant to most GNN architectures. Because the hash vectors add random projections into a new space, the appropriate embedding learned on this space can minimize the distortion with respect to the graph distance. Recent exceptions (Chami et al., 2019; Liu et al., 2019) focus on hyperbolic spaces rather than Euclidean, but appealing to the Nash Embedding Theorem (Nash, 1956) extends the arguments of this paper to those architectures.

In order to ensure that the mapping learned by the GNN algorithm is minimally distorted with respect to the graph distance metric, the graph distance must be explicitly incorporated into the training objective. In Section 5, we elaborate on how the loss function must be modified to achieve such an objective.

**Complexity Analysis.** Since IGNN augments the existing GNN architectures with hashed features, it behooves us to examine the complexity difference compared to these architectures. There are three sources of complexity changes when adopting this prescription. First, calculating the hash vectors incurs a cost of  $\mathcal{O}(Nn)$ , where  $N$  is the number of nodes and  $n$  is the dimension of the hash vectors. Adding the hash vectors introduces  $\mathcal{O}(n)$  additional model parameters, which introduce additional cost during both inference and back-propagation. There is a fixed cost of  $\mathcal{O}(N^3)$  of calculating the graph distances between the nodes for use in the loss function.<sup>2</sup> For a large graph, one may use an approximate shortest path algorithm (Henzinger et al., 2013) to avoid the cubic complexity.

## 5. Experiment

### 5.1. Methods

**Extending Input Representation.** We extend the input representation (either one-hot vectors or node features)  $\mathbf{x}_{v_i}$  for node  $v_i$  with fixed-length hash vectors

$$\mathbf{x}_{v_i}^{\mathcal{H}} = [\mathcal{H}(b_i \oplus 0), \mathcal{H}(b_i \oplus 1), \dots, \mathcal{H}(b_i \oplus n - 1)]^T \quad (3)$$

where  $b_i$  is a unique identifier for each node to achieve determinism and  $n$  denotes the desired length of the hash features. In all of our experiments, we adopt

$$\mathcal{H}(\cdot) = \text{MurmurHash3}(\cdot) / (2^{31} - 1) \quad (4)$$

<sup>2</sup>The same cost is needed in P-GNN models.

as the default hashing algorithm (Appleby) which hashes an arbitrary string into the range  $[-2^{31} - 1, 2^{31} - 1]$ . In essence, we provide a modular extension to all GNN algorithms by extending the input representation of each node to  $\mathbf{x}_{v_i}^* = \text{CONCAT}(\mathbf{x}_{v_i}, \mathbf{x}_{v_i}^{\mathcal{H}})$ . In contrast to the original input representation of the nodes  $\mathbf{x}_i$  that encode application-specific characteristics, the features  $\mathbf{x}_{v_i}^{\mathcal{H}}$  derived from hashing, spanning the space  $[-1, 1]^n$ , are designed to counterbalance the isomorphism between remote communities.

**Application Tasks.** We enable all GNN algorithms with the extended input representations to learn a mapping  $f : \mathcal{V} \times \mathcal{X} \rightarrow \mathcal{Z}$  based on the target similarity metric  $d_y(\mathbf{z}_{v_i}, \mathbf{z}_{v_j})$  determined by downstream application tasks, such as link prediction, pairwise node classification and so on. In particular, we focus on the following two prediction tasks.

- **Link Prediction:** The objective here is to model a similarity metric defined by  $d_y(\mathbf{z}_{v_i}, \mathbf{z}_{v_j}) = 1$  if  $(v_i, v_j) \in \mathcal{E}^+$  and 0 if  $(v_i, v_j) \in \mathcal{E}^-$ , where  $\mathcal{E}^+ \subset \mathcal{E}$  represents the set of positive edges and  $\mathcal{E}^- = \mathcal{V} \times \mathcal{V} - \mathcal{E}$  represents the set of negative edges sampled from the underlying graph  $\mathcal{G} = (\mathcal{V}, \mathcal{E})$ .

- **Pairwise Node Classification:** In this task, in addition to the graph  $\mathcal{G}$ , an exclusive node-set partition  $\{\mathcal{P}_1, \mathcal{P}_2, \dots, \mathcal{P}_M\} \subseteq \mathcal{V}$  is provided. The target similarity metric for this task is defined as  $d_y(\mathbf{z}_{v_i}, \mathbf{z}_{v_j}) = 1$  if  $\exists \ell (v_i \in \mathcal{P}_\ell \wedge v_j \in \mathcal{P}_\ell)$  and 0 otherwise.

Note that the subscript  $y$  in  $d_y(\cdot, \cdot)$  makes it explicit that the similarity is calculated at the output task level. We will introduce two more distances of similar kind related to the graph and the embedding space and hence it is important to make the notations for distances clear and distinct.

**Optimization over Extended Representation.** To generalize the learning task introduced in Section 3, most GNN algorithms seek to learn a mapping  $f(v_i, \mathcal{N}(v_i), \mathbf{x}_{v_i}, \{\mathbf{x}_{v_j} : v_j \in \mathcal{N}(v_i)\})$  where  $\mathcal{N}(v_i)$  is taken as a collection of one-hop or two-hop neighbors for node  $v_i$ . P-GNN, on the other hand, constructs the neighborhood a little differently by augmenting the set  $\mathcal{N}(v_i)$  with a set of anchor nodes  $\mathcal{S}$ . Note that this set of anchor nodes appear in the neighborhood of each node in the graph. In contrast, our approach seeks to learn a function with extended input representations that can be formally written as  $f(v_i, \mathcal{N}(v_i), \mathbf{x}_{v_i}^*, \{\mathbf{x}_{v_j}^* : v_j \in \mathcal{N}(v_i)\})$ .

As described by You et al. (2019), most GNN models can be formalized by the following optimization:

$$\min \mathbb{E}_{v_i, v_j, \mathcal{N}(v_i), \mathcal{N}(v_j)} [\mathcal{L}(d_z(f_{v_i}, f_{v_j}), d_y(\mathbf{z}_{v_i}, \mathbf{z}_{v_j}))] \quad (5)$$

where  $f_{v_i} = f(v_i, \mathcal{N}(v_i), \mathbf{x}_{v_i}, \{\mathbf{x}_{v_\ell} : v_\ell \in \mathcal{N}(v_i)\})$  and  $f_{v_j} = f(v_j, \mathcal{N}(v_j), \mathbf{x}_{v_j}, \{\mathbf{x}_{v_\ell} : v_\ell \in \mathcal{N}(v_j)\})$ . The random variables  $v_i, v_j, \mathcal{N}(v_i), \mathcal{N}(v_j)$  are all sampled from

the probability distribution  $p(\mathcal{V})$  over the set of vertices, dictated by some properties of the graph. Likewise, with a small modification to the neighborhood construction  $\mathcal{N}(v_i)$  for each node (i.e. extending every neighborhood with the anchor nodes), PGNN can also be shown to optimize the objective given above. Note that the subscripts in  $d_z(\cdot, \cdot)$  and  $d_y(\cdot, \cdot)$  are meant to distinguish between the similarity metrics in the embedding space and target metric space respectively.

In contrast, our approach optimizes for the composite loss function given by:

$$\min \mathbb{E}_{v_i, v_j, \mathcal{N}(v_i), \mathcal{N}(v_j)} [\mathcal{L}(d_z(f_{v_i}^*, f_{v_j}^*), d_y(\mathbf{z}_{v_i}, \mathbf{z}_{v_j}), d_{\mathcal{G}}(v_i, v_j))] \quad (6)$$

where  $f_{v_i}^* = f(v_i, \mathcal{N}(v_i), \mathbf{x}_{v_i}^*, \{\mathbf{x}_{v_\ell}^* : v_\ell \in \mathcal{N}(v_i)\})$  and  $f_{v_j}^* = f(v_j, \mathcal{N}(v_j), \mathbf{x}_{v_j}^*, \{\mathbf{x}_{v_\ell}^* : v_\ell \in \mathcal{N}(v_j)\})$ . Note that we have augmented the loss function with an extra term  $d_{\mathcal{G}}(v_i, v_j)$  that denotes the distance between node  $v_i$  and  $v_j$  according to the underlying graph  $\mathcal{G}$ . This explicit dependence on the graph distance is expected to guide the optimization to a point where the learned embeddings can have minimal distortion. Also note that the feature presentation in the above objective function accounts for the extended set of features.

To make the minimization problem above explicit, we propose the following objective function

$$\mathcal{L} = \lambda_{\text{BCE}} \mathcal{L}_{\text{BCE}} + \lambda_{\text{MSE}} \mathcal{L}_{\text{MSE}} \quad (7)$$

which has two parts – the usual task-specific target similarity loss term, which is the regular binary cross entropy (BCE) loss, and the new distance metric loss term, which is a mean-squared error (MSE) term. The BCE loss can be formalized as:

$$\begin{aligned} \mathcal{L}_{\text{BCE}} = & - \sum_{v_i \neq v_j} [d_y(\mathbf{z}_{v_i}, \mathbf{z}_{v_j}) \log \sigma(\langle \mathbf{z}_{v_i}, \mathbf{z}_{v_j} \rangle) \\ & + (1 - d_y(\mathbf{z}_{v_i}, \mathbf{z}_{v_j})) \log(1 - \sigma(\langle \mathbf{z}_{v_i}, \mathbf{z}_{v_j} \rangle))] \quad (8) \end{aligned}$$

Similarly, the distance metric can be characterized as:

$$\mathcal{L}_{\text{MSE}} = \sum_{v_i \neq v_j} [(1 - \langle \mathbf{z}_{v_i}, \mathbf{z}_{v_j} \rangle) / 2 - (1 - 1/d_{\mathcal{G}}(v_i, v_j)^\alpha)]^2 \quad (9)$$

where  $\alpha$  is a hyper-parameter that controls the shape of the distance transformation. In all of our experiments, we set  $\alpha = 1$ . A larger value of  $\lambda_{\text{MSE}}$  or  $\lambda_{\text{BCE}}$  favors the distance metric loss or the binary cross-entropy loss respectively. Interestingly, depending on the actual training task (i.e., link prediction, pairwise node classification, etc), these two losses might positively correlate. For example, for link prediction tasks, there exists a clear positive correlation between  $1 - d_y(\mathbf{z}_{v_i}, \mathbf{z}_{v_j})$  and  $(1 - 1/d_{\mathcal{G}}(v_i, v_j)^\alpha)$ .

## 5.2. Datasets

We conduct experiments on three real-world datasets – Communities, Email, and PPI.

- **Communities** (Watts, 1999) dataset is generated by first producing  $n = 20$  cliques of size  $k = 20$  each and then generating an edge to connect with an adjacent clique. To introduce some randomness, we connect cliques using an edge with a probability of 0.01. Furthermore, we use node-clique membership as the natural label for the node pair classification task.

- **Email** (Leskovec et al., 2007) is a collection of seven real-world email communication graphs with no node features. Each graph in this dataset has six communities and each node is labelled with the community it belongs to, which is used as the node pair classification label.

- **PPI** (Zitnik & Leskovec, 2017) network contains 1113 nodes and each node is equipped with a 29 dimensional feature vector. Each node represents a protein and an edge exists between two proteins if they interact with each other. Note that we only conduct the link prediction task for this dataset.

## 5.3. Experiment Setup

We consider the following baselines and their modifications to understand the impact of different modifications to the objective function used for graph embedding.

- **Baseline Models:** We consider GCN (Kipf & Welling, 2017), GraphSage (SAGE) (Hamilton et al., 2017a), Graph Attention Network (GAT) (Velickovi et al., 2018), Graph Isomorphism Network (GIN) (Xu et al., 2019), and P-GNN (You et al., 2019) as our baseline models without modification of either node features or loss function.

- **Baseline + Hash:** For this category of variations, we only endow each node with hashing based features.

- **Baseline + MSE:** For this category of variations, we modify the objective function in Equation 7 with losses from the target task metric and distance distortion.

- **Baseline + Both:** This is the combined version that includes the modified objective function and the input representation extension.

We evaluate the performance of all the models using the standard measure of classification performance, AUC-ROC, and a metric sensitive to distance, Kendall’s Tau (Kendall, 1948; Knight, 1966). Kendall’s Tau increases as distortion decreases. We use a variant of the Kendall’s Tau (KT) measure that adjusts for any ties. Given two lists of rankings,  $A$  and  $B$ , this measure is calculated as

$$\tau_b = \frac{(P - Q)}{\sqrt{(P + Q + T) \times (P + Q + U)}} \quad (10)$$

where  $P$  is the number of concordant pairs,  $Q$  is the number of discordant pairs and  $T$  ( $U$ ) is the number of ties in  $A$  ( $B$ ) only. A tie that occurs for a pair in both  $A$  and  $B$  is not counted in either  $T$  or  $U$ . We compare the rankings in the ascending order of graph distance and in the descending order of cosine similarity.

Table 1. Results for Communities and Email Dataset

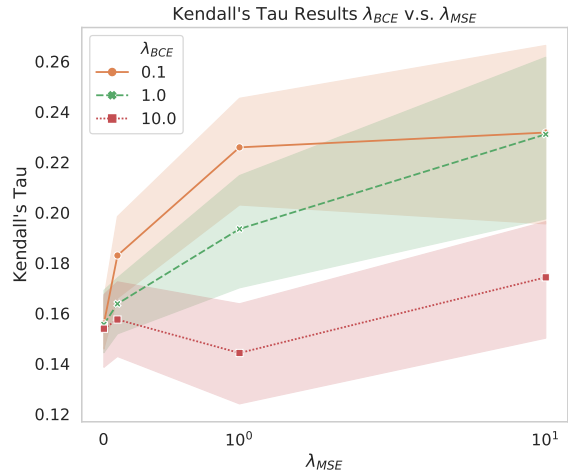
Model Variants	Communities				Email			
	Link Prediction		Pairwise Node Classification		Link Prediction		Pairwise Node Classification	
	AUC	Kendall's Tau	AUC	Kendall's Tau	AUC	Kendall's Tau	AUC	Kendall's Tau
GCN	0.977 ± 0.005	0.182 ± 0.038	0.988 ± 0.001	0.146 ± 0.015	0.709 ± 0.010	0.239 ± 0.025	0.518 ± 0.010	0.238 ± 0.008
GCN + Hash	0.986 ± 0.001	0.215 ± 0.001	0.992 ± 0.005	0.217 ± 0.002	0.767 ± 0.005	0.364 ± 0.008	0.681 ± 0.030	0.432 ± 0.002
GCN + MSE	0.986 ± 0.002	0.267 ± 0.003	0.992 ± 0.002	0.277 ± 0.003	0.721 ± 0.005	0.217 ± 0.004	0.575 ± 0.020	0.267 ± 0.050
GCN + Both	0.986 ± 0.003	<b>0.301 ± 0.002</b>	0.992 ± 0.002	<b>0.335 ± 0.003</b>	0.782 ± 0.016	<b>0.364 ± 0.002</b>	0.708 ± 0.020	<b>0.437 ± 0.002</b>
SAGE	0.986 ± 0.003	0.218 ± 0.003	0.993 ± 0.001	0.212 ± 0.015	0.571 ± 0.033	0.147 ± 0.011	0.538 ± 0.007	0.139 ± 0.012
SAGE + Hash	0.979 ± 0.004	<b>0.268 ± 0.029</b>	0.982 ± 0.006	0.257 ± 0.043	0.735 ± 0.000	0.361 ± 0.017	0.693 ± 0.010	0.428 ± 0.007
SAGE + MSE	0.985 ± 0.003	0.248 ± 0.004	0.994 ± 0.002	0.270 ± 0.038	0.557 ± 0.069	0.156 ± 0.030	0.533 ± 0.001	0.206 ± 0.033
SAGE + Both	0.986 ± 0.003	0.253 ± 0.002	0.993 ± 0.002	<b>0.280 ± 0.002</b>	0.769 ± 0.016	<b>0.363 ± 0.002</b>	0.744 ± 0.022	<b>0.433 ± 0.002</b>
GAT	0.981 ± 0.001	0.203 ± 0.028	0.989 ± 0.005	0.205 ± 0.006	0.538 ± 0.015	0.086 ± 0.009	0.507 ± 0.006	0.083 ± 0.018
GAT + Hash	0.919 ± 0.008	0.263 ± 0.014	0.975 ± 0.004	<b>0.334 ± 0.028</b>	0.758 ± 0.010	0.336 ± 0.010	0.725 ± 0.017	0.407 ± 0.004
GAT + MSE	0.983 ± 0.001	0.300 ± 0.069	0.989 ± 0.001	0.318 ± 0.004	0.550 ± 0.013	0.096 ± 0.001	0.528 ± 0.009	0.112 ± 0.001
GAT + Both	0.987 ± 0.003	<b>0.303 ± 0.002</b>	0.993 ± 0.002	0.324 ± 0.002	0.769 ± 0.015	<b>0.353 ± 0.002</b>	0.747 ± 0.200	<b>0.435 ± 0.002</b>
GIN	0.980 ± 0.002	0.241 ± 0.010	0.991 ± 0.002	0.213 ± 0.041	0.724 ± 0.008	0.402 ± 0.004	0.723 ± 0.032	0.479 ± 0.001
GIN + Hash	0.988 ± 0.007	0.272 ± 0.001	0.982 ± 0.006	0.250 ± 0.021	0.785 ± 0.007	0.443 ± 0.012	0.741 ± 0.001	<b>0.525 ± 0.001</b>
GIN + MSE	0.987 ± 0.003	0.290 ± 0.002	0.992 ± 0.002	0.301 ± 0.002	0.791 ± 0.012	0.429 ± 0.001	0.726 ± 0.012	0.482 ± 0.001
GIN + Both	0.987 ± 0.009	<b>0.432 ± 0.092</b>	0.984 ± 0.000	<b>0.365 ± 0.070</b>	0.808 ± 0.004	<b>0.452 ± 0.005</b>	0.774 ± 0.005	0.521 ± 0.007
P-GNN-F-2L	0.978 ± 0.007	0.334 ± 0.003	0.986 ± 0.001	0.346 ± 0.005	0.751 ± 0.040	0.503 ± 0.002	0.751 ± 0.013	0.576 ± 0.007
P-GNN-F-2L + Hash	0.978 ± 0.003	0.340 ± 0.000	0.988 ± 0.004	0.358 ± 0.000	0.769 ± 0.031	0.529 ± 0.007	0.734 ± 0.033	0.615 ± 0.006
P-GNN-F-2L + MSE	0.982 ± 0.004	0.338 ± 0.009	0.991 ± 0.002	0.357 ± 0.011	0.835 ± 0.016	0.516 ± 0.015	0.772 ± 0.016	0.609 ± 0.015
P-GNN-F-2L + Both	0.980 ± 0.104	<b>0.341 ± 0.072</b>	0.987 ± 0.077	<b>0.359 ± 0.071</b>	0.823 ± 0.040	<b>0.532 ± 0.056</b>	0.769 ± 0.030	<b>0.616 ± 0.006</b>
P-GNN-E-2L	0.965 ± 0.002	0.554 ± 0.017	0.981 ± 0.000	0.518 ± 0.018	0.792 ± 0.031	0.547 ± 0.011	0.735 ± 0.047	0.603 ± 0.013
P-GNN-E-2L + Hash	0.973 ± 0.006	<b>0.600 ± 0.004</b>	0.981 ± 0.001	0.576 ± 0.047	0.770 ± 0.030	0.549 ± 0.008	0.784 ± 0.020	<b>0.638 ± 0.001</b>
P-GNN-E-2L + MSE	0.985 ± 0.110	0.566 ± 0.161	0.990 ± 0.092	0.535 ± 0.152	0.765 ± 0.025	0.539 ± 0.010	0.772 ± 0.014	0.612 ± 0.007
P-GNN-E-2L + Both	0.982 ± 0.053	0.588 ± 0.013	0.994 ± 0.041	<b>0.607 ± 0.010</b>	0.775 ± 0.007	<b>0.550 ± 0.005</b>	0.753 ± 0.010	0.614 ± 0.000

Table 2. Results for PPI Dataset

Model Variants	Link Prediction	
	AUC	Kendall's Tau
GCN	0.798 ± 0.005	0.413 ± 0.010
GCN + Hash	0.810 ± 0.002	0.441 ± 0.007
GCN + MSE	0.760 ± 0.003	0.422 ± 0.005
GCN + Both	0.821 ± 0.001	<b>0.444 ± 0.005</b>
SAGE	0.809 ± 0.004	0.426 ± 0.015
SAGE + Hash	0.818 ± 0.003	<b>0.464 ± 0.012</b>
SAGE + MSE	0.804 ± 0.005	0.421 ± 0.012
SAGE + Both	0.812 ± 0.001	0.461 ± 0.002
GAT	0.798 ± 0.007	0.416 ± 0.012
GAT + Hash	0.818 ± 0.015	0.462 ± 0.010
GAT + MSE	0.789 ± 0.004	0.413 ± 0.012
GAT + Both	0.819 ± 0.005	<b>0.465 ± 0.012</b>
GIN	0.755 ± 0.014	0.442 ± 0.010
GIN + Hash	0.788 ± 0.024	0.450 ± 0.029
GIN + MSE	0.751 ± 0.012	0.432 ± 0.045
GIN + Both	0.789 ± 0.038	<b>0.460 ± 0.053</b>
P-GNN-F-2L	0.812 ± 0.007	0.375 ± 0.001
P-GNN-F-2L + Hash	0.823 ± 0.004	0.388 ± 0.005
P-GNN-F-2L + MSE	0.815 ± 0.014	0.372 ± 0.005
P-GNN-F-2L + Both	0.819 ± 0.007	<b>0.391 ± 0.010</b>
P-GNN-E-2L	0.772 ± 0.003	0.435 ± 0.004
P-GNN-E-2L + Hash	0.775 ± 0.014	0.426 ± 0.003
P-GNN-E-2L + MSE	0.792 ± 0.015	0.446 ± 0.005
P-GNN-E-2L + Both	0.798 ± 0.015	<b>0.454 ± 0.005</b>

#### 5.4. Hyper-parameter Selection

All of our experiments use PYTORCH (Paszke et al., 2019) with models implemented, when available, in the PYTORCH-GEOMETRIC package (Fey & Lenssen, 2019). For the GCN, SAGE, GIN, and GAT models, we use three hidden layers with 32 dimensions. For P-GNN, we use two hidden layers (-2L) with either truncated 2-hop (-F) or exact (-E) shortest path distance. We perform a hyper-parameter search with


 Figure 1. Impact of  $\lambda_{MSE}$  on KT

three possible values of the learning rate 0.0001, 0.001, and 0.01. The IGNN prescription introduces two new hyper-parameters – the dimension  $n$  of the hash vector and the strength  $\lambda_{MSE}$  associated with the MSE objective. In practice, setting  $n$  to the dimension of the observed node features works reasonably well. We also experiment with different values of  $\lambda_{BCE}$  and  $\lambda_{MSE}$  – 0, 0.1, 1.0, 10.0 – to understand their impact on AUC-ROC and KT. Figure 1 demonstrates the effect of  $\lambda_{MSE}$  on the KT measure for different values of  $\lambda_{BCE}$  when GCN algorithm is applied on the Communities dataset. One can observe that reducing  $\lambda_{BCE}$  and setting a slightly higher  $\lambda_{MSE}$  produce the best KT results with minimal effect on AUC-ROC. We use the best hyper-parameter set from the Email dataset and use that in the PPI dataset, as sweeping through all possible configurations of the hyper-parameters is quite expensive for the PPI dataset. We report

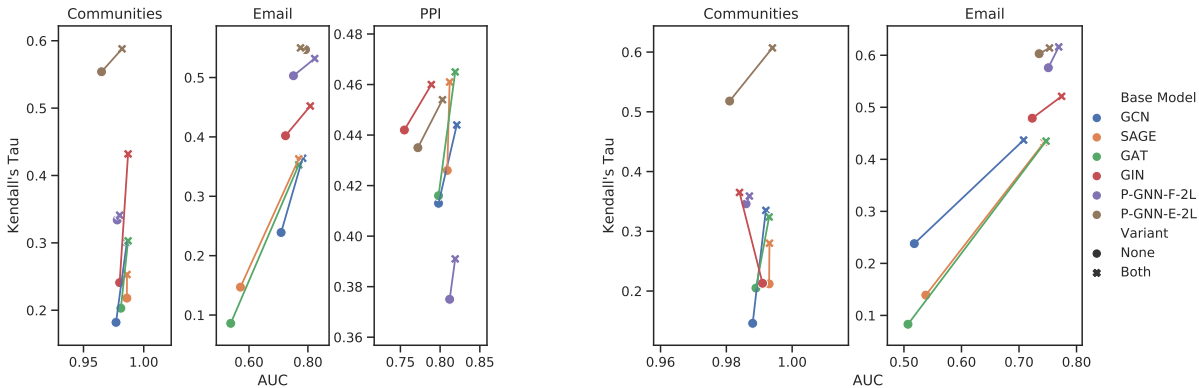


Figure 2. AUC-ROC vs KT for Link Prediction (Left) and Pairwise Node Classification (Right)

the test results using the hyper-parameter configurations that yield the best validation results.

### 5.5. Results

We present the results for the Communities, Email, and PPI datasets in Tables 1 and 2, respectively. Table 1 presents the AUC-ROC and Kendall’s Tau measures for the Communities and Email datasets for both the link prediction and pairwise node classification tasks for the four variants of each of the six model architectures we experiment with. Table 2 contains the AUC-ROC and KT for PPI for the link prediction task for the same set of model variants.

It is obvious from these results that adopting the IGNN technique improves KT for virtually all the datasets, tasks, and architectures, by as much as 400% in one case. In the Email dataset, we also see substantial improvement in the AUC-ROC, up to 43%. In the Communities dataset, the improvement is incremental, as most of the baseline models already have a very high AUC-ROC.

Figure 2 shows how AUC-ROC and KT evolve between the baseline and the “Both” variant of each model for the link prediction as well as the pairwise node classification task, allowing comparison of the improvement between different model architectures. In all cases, the IGNN models (“Both” variants) have an increase in KT measurement. In more than 93% (28 out of 30) of the cases, the AUC-ROC scores for the IGNN models are better than or as good as baseline models.

When reviewing the results for the Communities and Email datasets, which use one-hot encoded input features, we see that GCN, SAGE, and GAT have similar KT for both prediction tasks for the baseline models. This result is not surprising, as these architectures focus primarily on incorporating node features and are known to be challenged in distinguishing certain structural differences. All three architectures register substantial improvements when they are empowered with the IGNN technique. The variants associated with the GIN and P-GNN have notably higher baseline

performance, a result that is not surprising, as these architectures specifically aim to break structural isomorphisms and improve position awareness, respectively. Still, the improvement in KT is up to 70% for GIN and 17% for P-GNN variants.

In the PPI dataset where each node is attributed with a set of features, the situation is much different. The improvement in performance compared to the baselines is much lower than in the other datasets. The AUC-ROC improvement between baseline and the best IGNN variant is limited to 3% only, though we see improvement up to 9% in the KT measure. A notable exception is the P-GNN-F variant, which uses an approximate distance graph measure in the architecture (in contrast to the P-GNN-E variant, which uses the exact distance). This introduction of biased information likely results in lower performance. However, the fact that the architectures, such as GCN, SAGE, GAT, that focus primarily on node feature learning can achieve performance similar to the architectures explicitly taking advantage of structural or position information (GIN and P-GNN) strongly supports that the prescription presented in this paper enables these architectures to learn distance information.

### 6. Conclusion

We provide a prescription for training Isometric Graph Neural Networks using *any* GNN architecture, allowing these algorithms to compute node representations that remain faithful to graph distance. This prescription introduces minimal complexity overhead, allowing different architectures to maintain their respective advantages. We show that IGNNs improve performance over baselines in a variety of tasks in both the standard metric of AUC-ROC used for link prediction and the distance sensitive metric Kendall’s Tau.

## References

- Ahmed, A., Shervashidze, N., Narayanamurthy, S., Josifovski, V., and Smola, A. J. Distributed large-scale natural graph factorization. In *Proc. of WWW*, pp. 37–48, 2013.
- Alahi, A., Goel, K., Ramanathan, V., Robicquet, A., Fei-Fei, L., and Savarese, S. Social lstm: Human trajectory prediction in crowded spaces. In *Proc. of CVPR*, pp. 961–971, 2016.
- Appleby, A. Murmurhash3, 2016. URL: <https://github.com/aappleby/smhasher/wiki/MurmurHash3>.
- Banino, A., Barry, C., Uria, B., Blundell, C., Lillicrap, T., Mirowski, P., Pritzel, A., Chadwick, M. J., Degris, T., Modayil, J., et al. Vector-based navigation using grid-like representations in artificial agents. *Nature*, 557(7705):429, 2018.
- Battaglia, P. W., Hamrick, J. B., Bapst, V., Sanchez-Gonzalez, A., Zambaldi, V., Malinowski, M., Tacchetti, A., Raposo, D., Santoro, A., Faulkner, R., et al. Relational inductive biases, deep learning, and graph networks. *arXiv preprint arXiv:1806.01261*, 2018.
- Belkin, M. and Niyogi, P. Laplacian eigenmaps and spectral techniques for embedding and clustering. In *Proc. of NIPS*, pp. 585–591, 2002.
- Bourgain, J. On lipschitz embedding of finite metric spaces in hilbert space. *Israel Journal of Mathematics*, 52(1):46–52, 1985.
- Chami, I., Ying, Z., Ré, C., and Leskovec, J. Hyperbolic graph convolutional neural networks. In *Proc. of NIPS*, pp. 4869–4880, 2019.
- Chen, Z., Villar, S., Chen, L., and Bruna, J. On the equivalence between graph isomorphism testing and function approximation with gnns. In *Proc. of NIPS*, pp. 15868–15876, 2019.
- Cueva, C. J. and Wei, X.-X. Emergence of grid-like representations by training recurrent neural networks to perform spatial localization. In *Proc. of ICLR*, 2018.
- Fey, M. and Lenssen, J. E. Fast graph representation learning with PyTorch Geometric. In *ICLR Workshop on Representation Learning on Graphs and Manifolds*, 2019.
- Frankl, P. and Maehara, H. The johnson-lindenstrauss lemma and the sphericity of some graphs. *Journal of Combinatorial Theory, Series B*, 44(3):355 – 362, 1988.
- Gao, R., Xie, J., Zhu, S.-C., and Wu, Y. N. Learning grid cells as vector representation of self-position coupled with matrix representation of self-motion. In *Proc. of ICLR*, 2019.
- Gilmer, J., Schoenholz, S. S., Riley, P. F., Vinyals, O., and Dahl, G. E. Neural message passing for quantum chemistry. In *Proc. of ICML*, pp. 1263–1272, 2017.
- Grover, A. and Leskovec, J. node2vec: Scalable feature learning for networks. In *Proc. of KDD*, pp. 855–864, 2016.
- Hamilton, W., Ying, Z., and Leskovec, J. Inductive representation learning on large graphs. In *Proc. of NIPS*, pp. 1024–1034, 2017a.
- Hamilton, W. L., Ying, R., and Leskovec, J. Representation learning on graphs: Methods and applications. *arXiv preprint arXiv:1709.05584*, 2017b.
- Henzinger, M., Krinninger, S., and Nanongkai, D. Dynamic approximate all-pairs shortest paths: Breaking the  $o(mn)$  barrier and derandomization. In *2013 IEEE 54th Annual Symposium on Foundations of Computer Science*, pp. 538–547, 2013.
- Islam, M. A., Jia, S., and Bruce, N. D. B. How much position information do convolutional neural networks encode? In *Proc. of ICLR*, 2020.
- Johnson, W. B. and Lindenstrauss, J. Extensions of lipschitz mappings into a hilbert space. *Contemporary Mathematics*, 26: 189–205, 1984.
- Kendall, M. G. *Rank correlation methods*. Charles Griffin & Co. Ltd., London, 1948.
- Kipf, T. N. and Welling, M. Semi-Supervised Classification with Graph Convolutional Networks. In *Proc. of ICLR*, 2017.
- Knight, W. R. A computer method for calculating kendall’s tau with ungrouped data. *Journal of the American Statistical Association*, 61(314):436–439, 1966.
- Leskovec, J., Kleinberg, J., and Faloutsos, C. Graph evolution: Densification and shrinking diameters. *ACM transactions on Knowledge Discovery from Data (TKDD)*, 1(1):2–es, 2007.
- Liao, R., Li, Y., Song, Y., Wang, S., Hamilton, W., Duvenaud, D. K., Urtasun, R., and Zemel, R. Efficient graph generation with graph recurrent attention networks. In *Proc. of NIPS*, pp. 4257–4267, 2019.
- Linial, N., London, E., and Rabinovich, Y. The geometry of graphs and some of its algorithmic applications. *Combinatorica*, 15(2): 215–245, 1995.
- Liu, Q., Nickel, M., and Kiehl, D. Hyperbolic graph neural networks. In *Proc. of NIPS*, pp. 8228–8239, 2019.
- Mai, G., Janowicz, K., Yan, B., Zhu, R., Cai, L., and Lao, N. Multi-scale representation learning for spatial feature distributions using grid cells. In *Proc. of ICLR*, 2020.
- Maron, H., Ben-Hamu, H., Serviansky, H., and Lipman, Y. Provably powerful graph networks. In *Proc. of NIPS*, pp. 2153–2164, 2019.
- McFee, B. and Lanckriet, G. Partial order embedding with multiple kernels. In *Proceedings of the 26th Annual International Conference on Machine Learning*, pp. 721–728, 2009.
- Nash, J. The imbedding problem for riemannian manifolds. *Annals of Mathematics*, 63(1):20–63, 1956.
- Ou, M., Cui, P., Pei, J., Zhang, Z., and Zhu, W. Asymmetric transitivity preserving graph embedding. In *Proc. of KDD*, pp. 1105–1114, 2016.
- Pan, X., Shi, J., Luo, P., Wang, X., and Tang, X. Spatial as deep: Spatial cnn for traffic scene understanding. In *Proc. of AAAI*, 2018.
- Paszke, A. et al. Pytorch: An imperative style, high-performance deep learning library. In *Proc. of NIPS*, pp. 8024–8035, 2019.
- Perozzi, B., Al-Rfou, R., and Skiena, S. Deepwalk: Online learning of social representations. In *Proc. of KDD*, pp. 701–710, 2014.

- Srinivasan, B. and Ribeiro, B. On the equivalence between node embeddings and structural graph representations, 2019.
- Sugiyama, M. and Borgwardt, K. Halting in random walk kernels. In *Proc. of NIPS*, pp. 1639–1647, 2015.
- Sutskever, I., Vinyals, O., and Le, Q. Sequence to sequence learning with neural networks. *Proc. of NIPS*, 2014.
- Vaswani, A., Shazeer, N., Parmar, N., Uszkoreit, J., Jones, L., Gomez, A. N., Kaiser, Ł., and Polosukhin, I. Attention is all you need. In *Proc. of NIPS*, pp. 5998–6008, 2017.
- Veličković, P., Ying, R., Padovano, M., Hadsell, R., and Blundell, C. Neural execution of graph algorithms. In *Proc. of ICLR*, 2020.
- Velickovi, P., Cucurull, G., Casanova, A., Romero, A., Li, P., and Bengio, Y. Graph attention networks. In *Proc. of ICLR*, 2018.
- Vendrov, I., Kiros, R., Fidler, S., and Urtasun, R. Order-embeddings of images and language. In Bengio, Y. and LeCun, Y. (eds.), *4th International Conference on Learning Representations, ICLR 2016, San Juan, Puerto Rico, May 2-4, 2016, Conference Track Proceedings*, 2016. URL <http://arxiv.org/abs/1511.06361>.
- Watts, D. J. Networks, dynamics, and the small-world phenomenon. *American Journal of sociology*, 105(2):493–527, 1999.
- Weisfeiler, B. and Lehman, A. A. A reduction of a graph to a canonical form and an algebra arising during this reduction. *Nauchno-Technicheskaya Informatsia*, 2(9):12–16, 1968.
- Xiao, Y., Mehrotra, K. G., Allis, D. G., and Borer, P. N. A fast sorting algorithm for aptamer identification using deep sequencing. In *2014 IEEE/ACM International Conference on Advances in Social Networks Analysis and Mining (ASONAM)*, pp. 759–763, 2014.
- Xu, K., Hu, W., Leskovec, J., and Jegelka, S. How powerful are graph neural networks? In *Proc. of ICLR*, 2019.
- Yan, B., Walker, M., and Janowicz, K. A time-aware inductive representation learning strategy for heterogeneous graphs. In *Proceedings of the 15th International Workshop on Mining and Learning with Graphs (MLG'19) at KDD'19*, 2019.
- Yanardag, P. and Vishwanathan, S. Deep graph kernels. In *Proc. of KDD*, pp. 1365–1374, 2015.
- Yang, Y., Tong, Y., Ma, S., and Deng, Z.-H. A position encoding convolutional neural network based on dependency tree for relation classification. In *Proc. of EMNLP*, pp. 65–74, 2016.
- You, J., Ying, R., and Leskovec, J. Position-aware graph neural networks. In *Proc. of ICML*, pp. 7134–7143, 2019.
- Zeng, D., Liu, K., Lai, S., Zhou, G., and Zhao, J. Relation classification via convolutional deep neural network. In *Proc. of COLING*, pp. 2335–2344, 2014.
- Zitnik, M. and Leskovec, J. Predicting multicellular function through multi-layer tissue networks. *Bioinformatics*, 33(14): i190–i198, 2017.